

Composing an Answer Key for Weighing the Giants’ Photometric Redshifts

EMILY BIERMANN, ADVISED BY ANJA VON DER LINDEN AND RICARDO HERBONNET

(Received May 17, 2019)

Submitted to Stony Brook Astronomy

ABSTRACT

The Weighing the Giants galaxy cluster catalogs measure cluster masses and study cosmology using weak lensing methods. In order to do this they measure photometric redshifts (photo-z’s) of galaxies to determine whether they are in the cluster, foreground, or background. The objects are observed in several photometric bands and then a spectral template is shifted to best match the data and determine the “photometric redshift” (photo-z). Although the photo-z method requires less observing time and can measure fainter objects than spectroscopic redshifts, as required by cluster cosmology, photo-z’s are usually much less precise. In this paper I provide a test of the Weighing the Giants photo-z measurements by comparing them to spectroscopic redshifts from other catalogs. After ensuring the catalogs match to the same object, I compare the spec-z and photo-z measurements. Excluding outliers with $\Delta z = (z_p - z_s)/(1 + z_s) \leq 0.1$, the distribution has a mean bias of -0.002 and scatter $\sigma_{\Delta z} = 0.03$ with a 9.4% outlier rate. This is in agreement with previous results from [Kelly et al. \(2014\)](#) who also found a mean bias of -0.002 and scatter $\sigma = 0.029$. The bias and outlier fraction meet the goals for photometric redshifts set by LSST (a bias, $\mu < 0.003$ and an outlier rate below 10%) but the scatter ($\sigma < 0.02$) does not. I also investigate the photo-z’s probability distribution using a PIT (probability integral transform) value histogram taking the spectroscopic redshift as truth. PIT values measure which quantile the “true” value lies in. The result shows little bias in the photo-z measurement, but peaks at the ends of the PIT distribution suggest 8% are “catastrophic outliers” meaning their “true” redshifts lie outside the $p(z)$ probability curve which meets the goal for LSST.

1. INTRODUCTION

Galaxy clusters provide insight into the nature of large scale structure. By studying these massive objects we can learn about dark matter, dark energy and the cosmological history of the universe. We can study these objects with weak lensing techniques, a method that requires a large statistical sample of galaxies. We measure the average ellipticity of the galaxies. A non-zero average indicates the galaxies are being lensed. In this case the lens is a galaxy cluster and by studying the properties of the lensed images we can calculate the mass of the cluster. In weak lensing, it is important to differentiate between background and foreground objects by comparing their redshifts. However, due to the large sample size required for cluster cosmology these

redshifts must be found photometrically rather than using traditional spectroscopic techniques. In this paper I will discuss how these photometric redshifts (photo-z’s) are measured and compare the Weighing the Giants ([von der Linden et al. 2014](#)) photometric redshift $p(z)$ distributions ([Kelly et al. 2014](#)) in the galaxy cluster MACS0454.6-0305 to spectroscopic measurements from [Crawford et al. \(2011\)](#).

In this paper I first introduce some background knowledge on weak lensing and redshift measurements in Section 2. Next, in Section 3 I discuss the Weighing the Giants catalog, the [Crawford et al. \(2011\)](#) catalog where the spec-z’s are drawn from, and how the Weighing the Giants photo-z measurements are evaluated. In Section 4, I discuss matching the spec-z’s from [Crawford et al. \(2011\)](#) to the Weighing the Giants catalog. Then, in Section 5 I compare the photo-z’s point-estimator measurements and $p(z)$ distributions to the spec-z’s. Lastly, in Section 6 I discuss the results and compare them to

Corresponding author: Emily Biermann
emily.biermann@stonybrook.edu

LSST photo-z data simulations.

2. BACKGROUND

2.1. Galaxy Clusters

Only about 5% of a galaxy cluster's mass comes from galaxies and only 15% of the mass is hot gas. About 80% of a galaxy cluster's mass is in a massive dark matter halo (Schneider 2006). During the inflation era random quantum fluctuations were imprinted into the fabric of the universe and amplified by gravity's pull. This created an infall of mass and merging that gave way to the dark matter halos (Allen et al. 2011). Studying these objects gives us a greater understanding of the structure of the universe. The mass of these clusters can be measured using weak lensing techniques. Lensing occurs when a galaxy cluster's gravity distorts the path of light from a background galaxy. An observer will see distorted images of the background galaxy as shown in Figure 1. By measuring this distortion one can determine the mass of the lens given the distance to the source and lensing object.

2.2. Weak Lensing

Lensing can produce very powerful and obvious effects such as the “Einstein Ring” in Figure 1. Clearly, this object is distorted from its original shape. Sometimes lensing effects are not quite so obvious. Take Figure 2, a simulation of lensed background galaxies for example. Clearly these objects are distorted but the effects are much less dramatic than the Einstein Ring. This is called “weak lensing”. In the top right panel of Figure 2 it is easy to see these objects are distorted because their original shape is known. Unfortunately this is not the reality when observing lensed galaxies. Galaxies come in all sorts of shapes and sizes and what we observe depends on the galaxy's orientation relative to our line of sight. Therefore, in practice it is very difficult to determine if an observation includes lensed features or simply randomly oriented galaxies. This is shown in the bottom panel of Figure 2 where shape noise of galaxies is added to the simulation. Luckily, one can still determine the objects are being lensed due to the objects' tangential alignment to the lensing mass.

In general (that is, for both weak and strong lensing effects) the local approximation of the transformation between lensed (x_l, y_l) and unlensed (x_u, y_u) angular coordinates is given by the following (Mandelbaum 2018):

$$\begin{pmatrix} x_u \\ y_u \end{pmatrix} = \begin{pmatrix} 1 - \gamma_1 - \kappa & -\gamma_2 \\ -\gamma_2 & 1 + \gamma_1 - \kappa \end{pmatrix} \begin{pmatrix} x_l \\ y_l \end{pmatrix}, \quad (1)$$

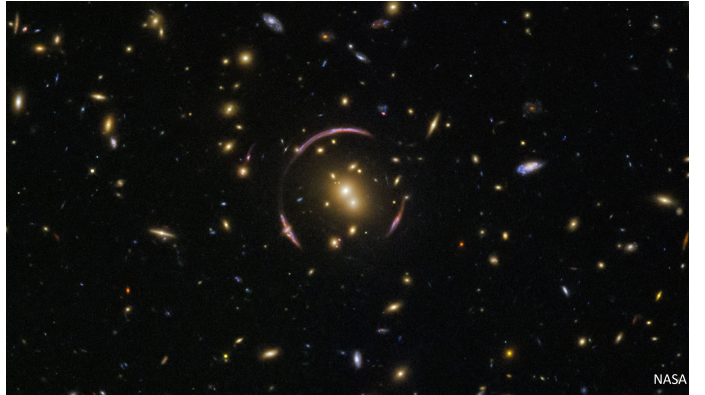


Figure 1. Hubble image of the galaxy cluster SDSS J0146-0929. The cluster is strongly lensing a background galaxy into these large circular arcs. This particular distortion pattern is called an “Einstein Ring” and occurs when the source object lies directly behind the lens. [image credit: [Hille and ESA/Hubble \(2018\)](#)]

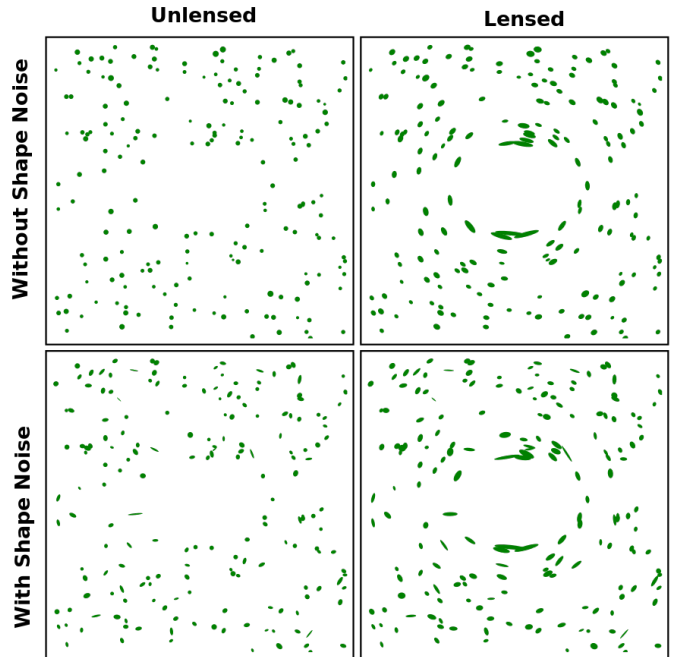


Figure 2. Simulation of weak lensing. The top panels show the unlensed and lensed galaxies without “shape noise”. The bottom panels show the same simulation with galaxies of varying ellipticity. In the left panels, even with varying shape, the average ellipticity of the galaxies is zero. On the right the galaxies are tangentially aligned with the lensing mass and therefore the average ellipticity is non-zero. [image credit: [Wikipedia user TallJimbo \(2008\)](#)]

where γ_1 and γ_2 are components of the shear. The shear describes the stretching of the image. The convergence, κ describes the change in the image's size and brightness and is defined as the projected matter over density

(Mandelbaum 2018).

Weak lensing provides a direct measurement of the total matter in a galaxy cluster without the need of a “baryonic tracer” (von der Linden et al. 2014). Other methods rely on visible matter for an estimate of the mass but this does not directly measure the mass of dark matter in a cluster. Unfortunately, weak lensing is a noisy phenomenon. The shear is small compared to random orientations of galaxies (Mandelbaum 2018) so one must gain a great understanding of statistical biases in order to perform a measurement. This comes from analyzing weak lensing of many galaxy clusters to study shear dependencies, cluster mass, the distance to the source and lensing cluster and cosmology, as well as observational biases, shear measurement and redshift measurements (von der Linden et al. 2014; Kelly et al. 2014; Applegate et al. 2014). Also, weak lensing only measures the projected 2D mass of the cluster. The projection can be converted to a 3D mass by fitting a spherically symmetric density model to the shear profile. Depending on the line of sight this may under or over estimate the mass so N-body simulations are used to uncover the bias and scatter (R. Becker and V. Kravtsov 2011).

2.3. Measuring Distances

Measuring the redshift tells us how far away objects are and therefore distinguishes whether the galaxy is in the background, foreground, or within the cluster. Redshift is a product of the expanding universe. As light travels to a distant observer the fabric of the universe expands. This causes the wavelength of the light to elongate. Therefore the spectrum of a distance object will be shifted to the red with respect to laboratory measurements. Redshift, z is defined as

$$z = \frac{\lambda_{\text{obs}} - \lambda_{\text{rest}}}{\lambda_{\text{rest}}} \quad (2)$$

where λ_{obs} is the observed wavelength and λ_{rest} is the rest frame wavelength.

If the expansion rate and other cosmological properties are known then the redshift can be converted into an angular diameter distance. This measures distance with respect to the apparent size of the object. The angular diameter distance, D_A is (Schneider 2006),

$$D_A = \frac{1}{1+z} \frac{c}{H_0} \int_0^z \frac{1}{E(z')} dz, \quad (3)$$

where,

$$E(z) = \sqrt{\Omega_m(1+z)^3 + \Omega_\kappa(1+z)^2 + \Omega_\Lambda}, \quad (4)$$

and H_0 is the Hubble constant, c is the speed of light, and Ω_m , Ω_κ , and Ω_Λ are the dimensionless mass density, curvature, and dark energy density of the universe, respectively. Given a redshift and cosmological parameters one can determine the distance to objects.

2.4. Photometric Redshift

Traditionally redshift is measured by observing the spectrum of an object and determining how far known emission or absorption lines are shifted. This is called a spectroscopic redshift, or “spec-z”. However, measuring spectra is a time-consuming process. The light is dispersed through a slit so only a fraction of the light is detected. Therefore the object must be observed for a much longer time than photometric observations. Also, only one object can be observed for each slit. Photometric redshifts (“photo-z”) provide a cheaper alternative. Observing a galaxy cluster using different filters provides a measurement of the flux of each object in the field of view at a specific spectral band as shown in Figure 3 (Padmanabhan et al. 2007). These can then be compared to known spectra at various redshift to find the redshift of the galaxy. This process is called “template fitting” (Schneider 2011). The spectrum mostly depends on the age of the galaxy. Older, redder, galaxies will have similar spectra and likewise newer, bluer galaxies will have similar spectra. Therefore, a limited set of templates can describe the majority of galaxies. The number of templates available and the lack of a continuous spectrum in the data still limit the accuracy of this process but it is much easier to measure these photo-z’s than spec-z’s from a continuous spectra.

3. METHODS

3.1. Weighing the Giants Catalog

The Weighing the Giants (WTG) project measured weak-lensing masses of X-ray luminous galaxy clusters using wide-field imaging with the Subaru and CFHT telescopes with the goal of improving mass calibration of cluster observables used to learn about cosmological parameters (von der Linden et al. 2014; Kelly et al. 2014; Applegate et al. 2014; Mantz et al. 2014; Mantz et al. 2016). In order to accommodate a large number of objects they measured photo-z’s rather than spec-z’s and for each cluster they took observations in three to five bands. Since these measurements, many spectroscopic redshifts of galaxies within these clusters have been measured. In this paper I compare the photo-z’s from the Weighing the Giants catalog to spec-z’s from “Spectroscopy of Luminous Compact Blue Galaxies in Distant Clusters” by Crawford et al. (2011) of the galaxy

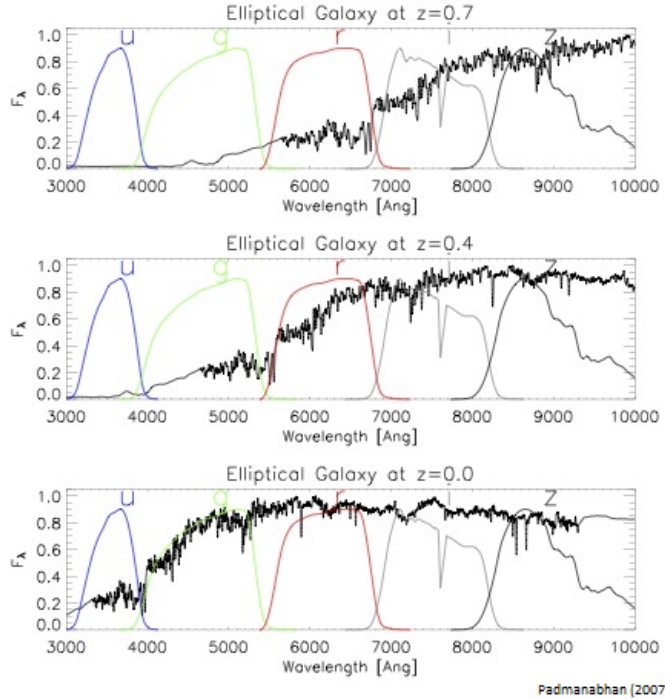


Figure 3. Spectrum of an elliptical galaxy (black) in u, g, r, i, and z bands (blue, green, red, grey, and black respectively). Observing the galaxy in each band provides 5 “data-points” of the full spectrum. A spectrum template is fitted to the data to find the redshift. [image credit: Padmanabhan et al. (2007)]

cluster MS0451.6-0305.

3.2. Photo-z PDF's

Simply citing a single point estimator of a photo-z measurement does not give an accurate representation of the data as this biases mass measurements. Rather, one must provide a redshift probability density function, referred to as either PDF or $p(z)$ which result in nearly unbiased mass measurements (Applegate et al. 2014). This is a posterior probability distribution of the photo-z measurement. The distribution shows how likely the redshift is to be a certain value given prior constraints and the data used to calculate the quantity (Schmidt et al. 2019). In this case, the data includes the flux in each spectral band of the object. The $p(z)$ distribution for each object was calculated by the WTG collaboration (Kelly et al. 2014). This paper will determine the accuracy of the ensemble of $p(z)$'s.

To do so I use the probability integral transform (PIT), defined as (Schmidt et al. 2019)

$$\text{PIT} = \int_{-\infty}^{z_{\text{true}}} p(z) dz, \quad (5)$$

where z_{true} is defined as the spectroscopic redshift. This equation determines the quantile of z_{true} within the $p(z)$ distribution. If the $p(z)$ distributions match the true redshift a histogram of PIT values will be flat. PIT values at either 0 or 1 represent “catastrophic failures” (Schmidt et al. 2019) which indicates the true redshift is completely outside the photo-z probability distribution.

Quantile-quantile, or QQ plots compare the quantiles of two distributions. In this paper I will present a QQ plot that compares the PIT values to quantiles from a uniform distribution. As stated, we expect the distribution to be flat. Therefore, the theoretical quantile distribution is an even distribution between zero and one.

4. DATA

The Weighing the Giants catalog for MACS0454 includes photo-z's for 125,916 objects. The telescope, camera, and filters used to measure the photo-z's are listed in table 1. The photo-z's were estimated using the Bayesian BPZ code (Kelly et al. 2014; Benitez 2000; Coe et al. 2006). The Crawford et al. 2011 data come from the DEIMOS spectrograph on the Keck II telescope as well as all literature measurements up until 2011. Most of these measurements are from Moran et al. (2007). The catalog includes spec-z's for 1,455 galaxies.

Camera	Telescope	Filter Name
SuprimeCam	Subaru	Johnson B -band (B_J) Johnson V -band (V_J) Cousins R -band (R_C) SDSS i -band (i^+) SDSS z -band (z^+)
MegaPrime	CFHT	SDSS u -band (u^*) SDSS g -band (g^*) SDSS r -band (r^*) SDSS i -band (i^*) SDSS z -band (z^*)
CFH12K	CFHT	Johnson B -band (B_{12}) Cousins I -band (I_{12})

Table 1. Filters used in Weighing the Giants photometric redshift measurements. [von der Linden et al. (2014)]

I used the astrophysics catalog tool topcat (Taylor 2005) to match the objects in the spec-z catalog from Crawford et al. (2011) to the Weighing the Giants Catalog of the galaxy cluster MACS0454. I used the version of the WTG Catalog which includes all detected objects

in order to match all observed objects to the Crawford catalog and reduce the likelihood of false matches. I cut all Crawford objects with a spec-z less than 0.01 as these are likely stars.

Because the WTG objects are from photometric observations, we expect the Crawford objects to be a subset of this catalog. I first matched the objects within a radius of one arcsecond and ± 1 in m_R . This resulted in a 65% match of the Crawford catalog to WTG. Many of the objects did not match due to a difference in astrometry within the Crawford catalog. This catalog contains spectroscopy from many different studies. One of the subsets of objects contained a radial shift in position with respect to the image center compared to the WTG objects. In order to fix this I repeated the matching process on the remaining objects with a three arcsecond radius. The magnitude cut allows insurance that the objects are matched correctly (see Figure 4). Combined, the two matches had 82% efficiency. All objects may not have matched due to masked areas in the WTG catalog.

Figure 4 compares the R-band magnitude from the Crawford and WTG catalogs for each matched object. If the objects are perfectly matched the magnitudes from each catalog will match as well within variations from differing measurement techniques. Therefore, this plot can tell us whether or not all objects were matched correctly.

5. RESULTS

5.1. Photometric and Spectroscopic Redshift Comparison

Figure 5 compares the photo-z's and spec-z's of each object. If the spec-z's and photo-z's were in perfect agreement all points would lie on the one-to-one line and in the “zero” bin of the histogram. The histogram and Gaussian fit includes all objects with

$$\Delta z \equiv (z_p - z_s)/(1 + z_s) \leq 0.1, \quad (6)$$

where z_p is the photometric redshift and z_s is the spectroscopic redshift. This cut excludes outliers which accounted for 9.4% of all objects. These photo-z's are measured with a scatter of $\sigma_{\Delta z} = 0.03$ and a bias, $\mu = -0.002$. A similar analysis by Kelly et al. (2014) yielded a similar measurement of $\mu = -0.002$ and $\sigma = 0.029$ for the same cluster. The photometric redshift goals for LSST are as follows: $\sigma_z < 0.02(1+z)$, 3σ outlier rate below 10% and bias below 0.003 (Schmidt et al. 2019). The measurements presented here meet the

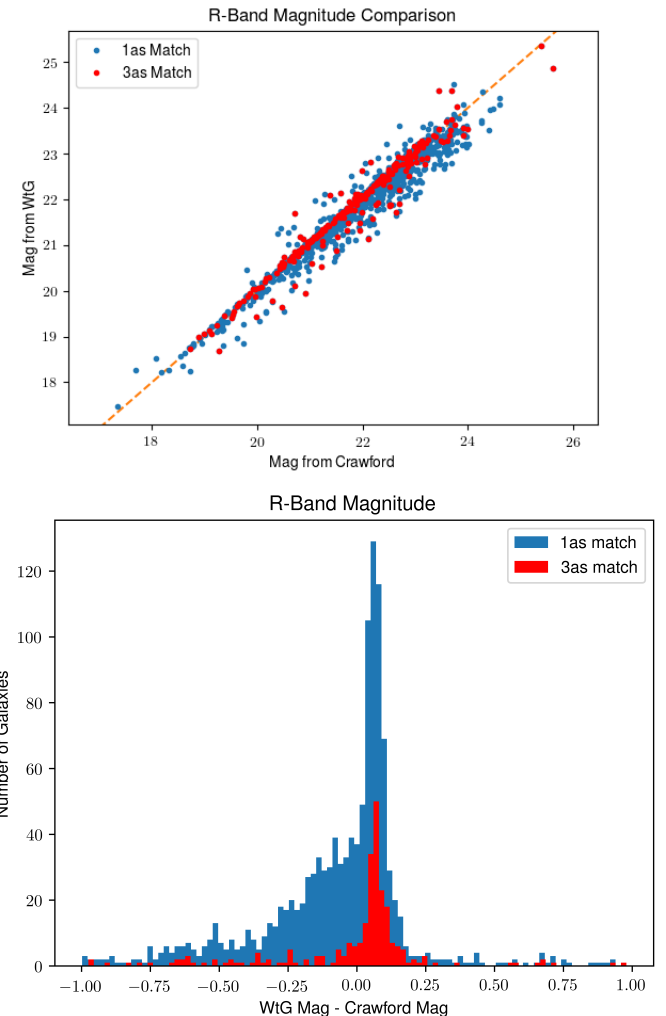


Figure 4. R-Band magnitude comparison of the Weighing the Giants and Crawford et al. catalogs. The top panel plots the R-band magnitude from the Weighing the giants catalogs (y-axis) and the Crawford et al. catalog (x-axis) for each object as well as the one-to-one line (dashed orange). The bottom panel shows the histogram of the residual between the two magnitudes for each object. The objects matched with a 1as radius are blue and the objects matched with a 3as radius are red. These magnitude comparisons indicates whether or not the objects are matched correctly between the two catalogs.

outlier rate and bias goal but the scatter is about 33% too large.

5.2. QQ Plot and PIT Values

Since not all of the photo-z's have a Gaussian probability distribution (see Figure 6), a single point estimator (as plotted in Figure 5) does not fully describe the measurement. Rather, we use PIT values and QQ

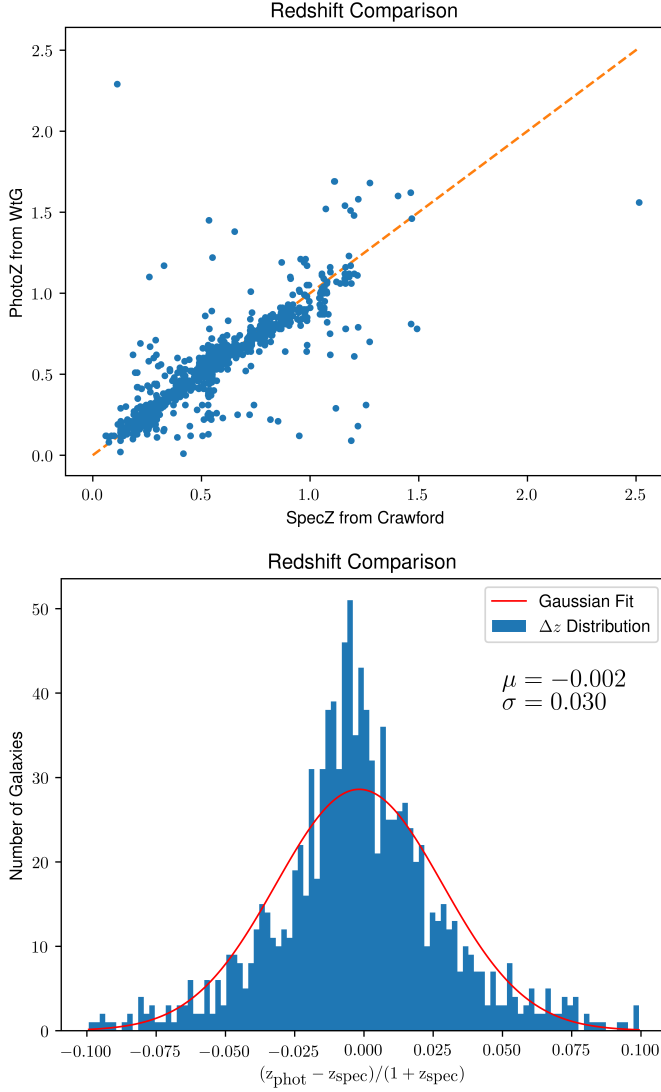


Figure 5. Photo-z and spec-z comparison for Weighing the Giants objects. The top panel plots the photometric and spectroscopic redshifts for each object (blue circles) as well as the one-to-one line (dashed orange). The bottom panel shows the distribution of $\Delta z = (z_p - z_s)/(1+z_s)$ with outliers, $\Delta z > 0.1$ removed (blue) and the Gaussian fit (red) defined by a mean bias $\mu = -0.002$ and scatter $\sigma_{\Delta z} = 0.03$.

plots to compare the photo-z's probability distributions to the “true” (spectroscopic) redshift. Figure 7 shows the PIT values and quantile-quantile (QQ) plot residuals which indicate how well the photo-z's are calculated relative to the spec-z's. The spec-z's are taken to be the “true redshift” because they are measured to a much greater precision and accuracy than photo-z's as explained in the introduction. The x-axis of the plot is the quantile of the spectroscopic redshift (z_{true}) within the posterior probability distribution of the photometric redshift for each object. Figure 6 shows some examples

of these posterior distributions and the “true” spectroscopic redshift. On the top panel of figure 7, the y-axis is the number of objects with a true redshift within the given quantile. For a perfect match this would be a flat distribution. The bottom panel plots the residual between the PIT values, Q_{data} , and the quantiles from a uniform distribution, Q_{theory} : $\Delta Q = Q_{\text{data}} - Q_{\text{theory}}$.

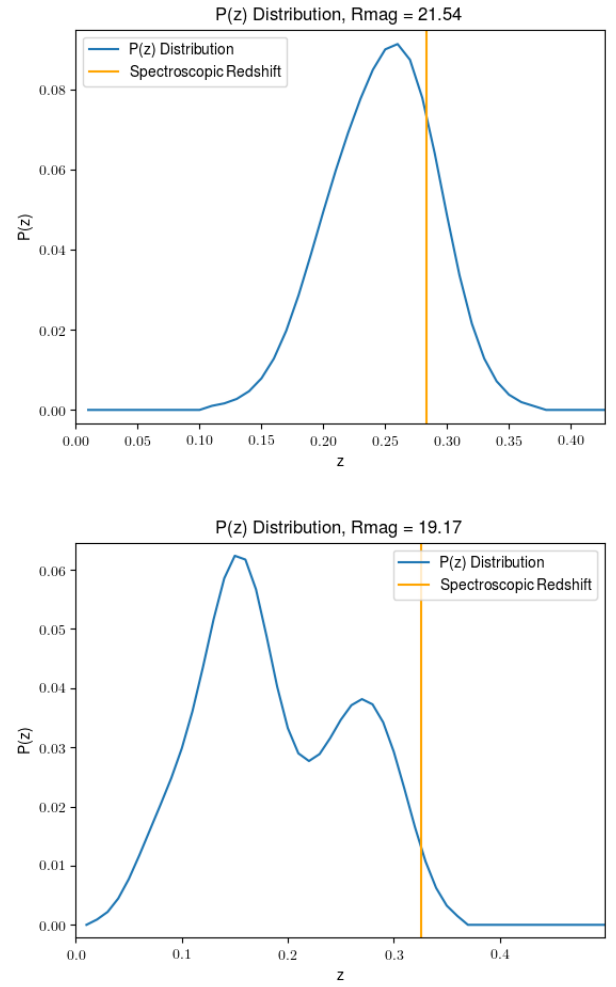


Figure 6. $p(z)$ distributions for two Weighing the Giants objects. The top panel shows a well-behaved, gaussian distribution. The bottom panel shows an example of a non-gaussian $p(z)$ thus demonstrating the need to consider the full distribution and not simply single point estimators in this analysis.

The sharp peaks at the 0 and 1 in the PIT histogram indicate “catastrophic failures” in the photometric redshift distribution (Schmidt et al. 2019). In these cases the “true” redshift lies outside the probability distribution. Luckily, the number of such catastrophic failures

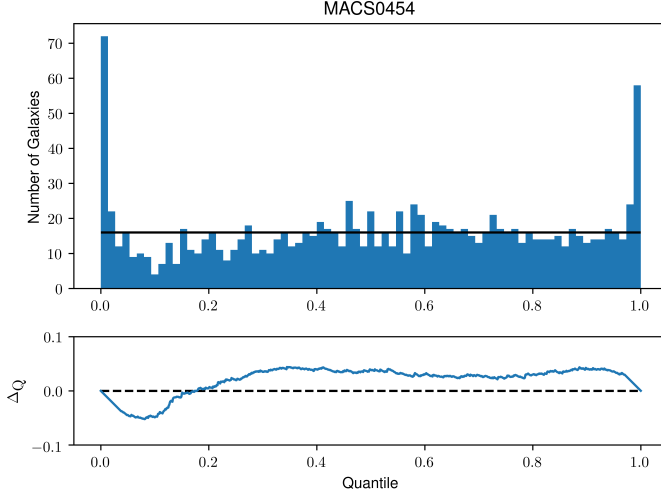


Figure 7. The top panel shows the PIT value distribution of Weighing the Giants photometric redshifts taking z_{true} to be the spectroscopic redshift (blue). The solid black line gives the theoretical, even distribution. All objects above this line in the zero and one bins indicate catastrophic failures where the true redshift is outside of the $p(z)$ distribution. The catastrophic failures make up about 8% of the entire distribution. The bottom panel plots the residual between the PIT quantiles and the theoretical quantiles from an even distribution, $\Delta Q = Q_{\text{data}} - Q_{\text{theory}}$ (blue). The dashed black line is at zero.

only accounts for 8% of all objects which meets the goals of LSST (Schmidt et al. 2019) and indicate less outliers than the point-estimator comparison (section 5.1). The histogram is also relatively flat indicating little bias in the photo-z measurement.

The LSST-DESC Photometric Working Group performed a similar analysis on idealized simulations of photometric redshift PDFs using twelve different photo-z measurement codes (Schmidt et al. 2019). Their results are shown in figure 8. The Weighing the Giants photo-z PDF's compare similarly to and, in some cases, better than these idealized results.

6. CONCLUSIONS

Weak lensing is very useful for measuring the mass of galaxy clusters but due to the statistical nature of the measurement many galaxies behind the cluster must be studied. Weak lensing also requires us to differentiate between background and foreground galaxies using a redshift in order to determine which galaxies are being lensed and which galaxies are in the cluster itself. However, due to the large number and faintness of these galaxies, spectroscopy is not a feasible method of measuring redshift. Instead, the galaxies are observed in many optical bands creating a “spectrum” with a small

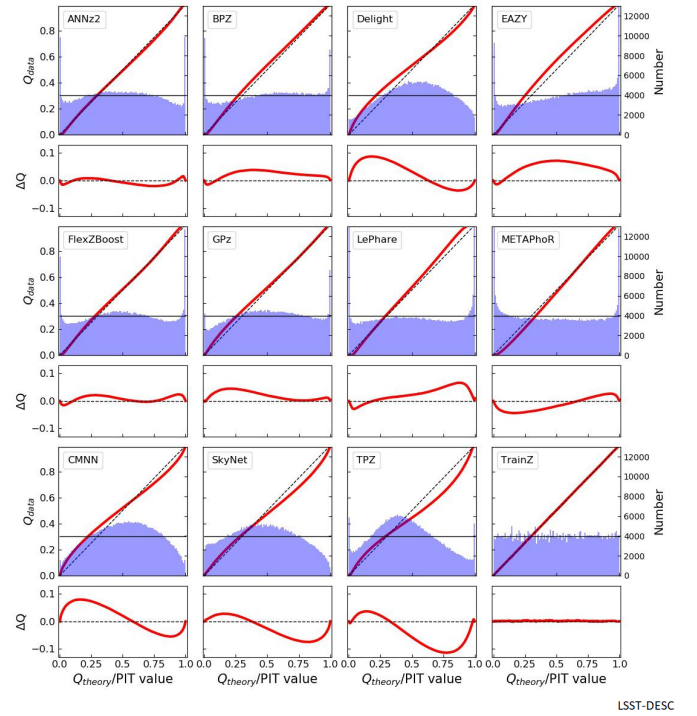


Figure 8. LSST-DESC PIT histograms and QQ plots of photo-z PDF distributions from idealized data simulations. The top panels for each code show the PIT histogram (blue) and QQ plot of the PIT distribution and theoretical, even distribution between zero and one (red). The solid black line shows an even distribution on the histogram. The bottom panels plot $\Delta Q = Q_{\text{data}} - Q_{\text{theory}}$ (red) and the zero-line (dashed black). These plots provide a comparative reference for the Weighing the Giants photo-z PIT histogram and QQ plot. [image credit: Schmidt et al. (2019)]

number of data points. Galaxy spectra templates are fitted to the data to measure the “photometric redshift”. Such redshifts were measured for galaxies in the fields of Weighing the Giants clusters.

I provided a check for these photo-z’s using spectroscopic redshifts from the Crawford et al. catalog. After matching the objects in each catalog, I found a mean bias of $\Delta z = (z_p - z_s)/(1 + z)$ with outliers $\Delta z > 0.1$ removed to be -0.002 and accuracy $\sigma_{\Delta z} < 0.03$ which is consistent with previous work by (Kelly et al. 2014) and with the bias and outlier rate goals of LSST. I investigated the accuracy of the photo-z’s probability distributions by finding the PIT values for each galaxy. The distribution shows little bias in the photometric redshift $p(z)$ distributions but there are some catastrophic outliers where the “true” redshift is outside the probability distribution entirely. This result is comparable, and in some cases better than photo-z reconstruction

on simulated data from LSST-DESC. This is a positive result that indicates the photo-z's in this analysis are correctly measured except for a small number of outliers

accounting for 8% of the measurements. This fraction of outliers meets the goal set by LSST.

REFERENCES

- Steven W. Allen, August E. Evrard, and Adam B. Mantz. Cosmological parameters from observations of galaxy clusters. *Annual Review of Astronomy and Astrophysics*, 49(1):409–470, 2011.
<https://doi.org/10.1146/annurev-astro-081710-102514>. URL
<https://doi.org/10.1146/annurev-astro-081710-102514>.
- Douglas E. Applegate, Anja von der Linden, Patrick L. Kelly, Mark T. Allen, Steven W. Allen, Patricia R. Burchat, David L. Burke, Harald Ebeling, Peter Capak, Oliver Czoske, David Donovan, Adam Mantz, and R. Glenn Morris. Weighing the Giants II. Improved calibration of photometry from stellar colours and accurate photometric redshifts. *Monthly Notices of the Royal Astronomical Society*, 439(1):28–47, 02 2014. ISSN 0035-8711. <https://doi.org/10.1093/mnras/stt1946>. URL <https://doi.org/10.1093/mnras/stt1946>.
- Rachel Mandelbaum. Weak lensing for precision cosmology. *Annual Review of Astronomy and Astrophysics*, 56(1):393–433, 2018.
<https://doi.org/10.1146/annurev-astro-081817-051928>. URL
<https://doi.org/10.1146/annurev-astro-081817-051928>.
- Adam B. Mantz, Anja von der Linden, Steven W. Allen, Douglas E. Applegate, Patrick L. Kelly, R. Glenn Morris, David A. Rapetti, Robert W. Schmidt, Saroj Adhikari, Mark T. Allen, Patricia R. Burchat, David L. Burke, Matteo Cataneo, David Donovan, Harald Ebeling, Sarah Shandera, and Adam Wright. Weighing the giants IV. Cosmology and neutrino mass. *Monthly Notices of the Royal Astronomical Society*, 446(3):2205–2225, 11 2014. ISSN 0035-8711.
<https://doi.org/10.1093/mnras/stu2096>. URL
<https://doi.org/10.1093/mnras/stu2096>.
- Dan Coe, Narciso Benítez, Sebastián F. Sánchez, Myungkook Jee, Rychard Bouwens, and Holland Ford. Galaxies in the hubble ultra deep field. i. detection, multiband photometry, photometric redshifts, and morphology. *The Astronomical Journal*, 132(2):926–959, jul 2006. <https://doi.org/10.1086/505530>. URL
<https://doi.org/10.1086%2F505530>.
- S. M. Crawford, G. D. Wirth, M. A. Bershady, and K. Hon. Spectroscopy of Luminous Compact Blue Galaxies in Distant Clusters. I. Spectroscopic Data. *ApJ*, 741:98, November 2011.
<https://doi.org/10.1088/0004-637X/741/2/98>.
- Karl Hille and ESA/Hubble. Hubble finds an einstein ring. *NASA*, Apr 2018. URL
<https://www.nasa.gov/image-feature/goddard/2018/hubble-finds-an-einstein-ring>.
- Patrick L. Kelly, Anja von der Linden, Douglas E. Applegate, Mark T. Allen, Steven W. Allen, Patricia R. Burchat, David L. Burke, Harald Ebeling, Peter Capak, Oliver Czoske, David Donovan, Adam Mantz, and R. Glenn Morris. Weighing the Giants II. Improved calibration of photometry from stellar colours and accurate photometric redshifts. *Monthly Notices of the Royal Astronomical Society*, 439(1):28–47, 02 2014. ISSN 0035-8711. <https://doi.org/10.1093/mnras/stt1946>. URL <https://doi.org/10.1093/mnras/stt1946>.
- Adam B. Mantz, Steven W. Allen, R. Glenn Morris, Anja von der Linden, Douglas E. Applegate, Patrick L. Kelly, David L. Burke, David Donovan, and Harald Ebeling. Weighing the giants V. Galaxy cluster scaling relations. *Monthly Notices of the Royal Astronomical Society*, 463(4):3582–3603, 09 2016. ISSN 0035-8711.
<https://doi.org/10.1093/mnras/stw2250>. URL
<https://doi.org/10.1093/mnras/stw2250>.
- Sean M. Moran, Richard S. Ellis, Tommaso Treu, Graham P. Smith, R. Michael Rich, and Ian Smail. A wide-field survey of two $z \sim 0.5$ galaxy clusters: Identifying the physical processes responsible for the observed transformation of spirals into s0s. *The Astrophysical Journal*, 671(2):1503–1522, dec 2007.
<https://doi.org/10.1086/522303>. URL
<https://doi.org/10.1086%2F522303>.

Nikhil Padmanabhan, David J. Schlegel, Uro Seljak, Alexey Makarov, Neta A. Bahcall, Michael R. Blanton, Jonathan Brinkmann, Daniel J. Eisenstein, Douglas P. Finkbeiner, James E. Gunn, David W. Hogg, eljko Ivezi, Gillian R. Knapp, Jon Loveday, Robert H. Lupton, Robert C. Nichol, Donald P. Schneider, Michael A. Strauss, Max Tegmark, and Donald G. York. The clustering of luminous red galaxies in the Sloan Digital Sky Survey imaging data. *Monthly Notices of the Royal Astronomical Society*, 378(3):852–872, 06 2007. ISSN 0035-8711. URL <https://doi.org/10.1111/j.1365-2966.2007.11593.x>. URL <https://doi.org/10.1111/j.1365-2966.2007.11593.x>.

Matthew R. Becker and Andrey V. Kravtsov. On the accuracy of weak lensing cluster mass reconstructions. *Astrophysical Journal - ASTROPHYS J*, 740, 8 2011. URL <https://doi.org/10.1088/0004-637X/740/1/25>.

Samuel Schmidt, Alex Malz, John Soo, Massimo Brescia, Stegano Cavaudi, Giuseppe Longo, Ibrahim Almosallam, Melissa Graham, Andrew Connolly, Efran Nourbakhsh, Johann Cohen-Tanugi, Hugo Tranin, Peter Freeman, Kartheik Iyer, Matt Jarvis, J. Bryce Kalmbach, Eve Kovacs, Joseph DeRose, Risa Wechsler, Ofer Lahav, Ann Lee, Christopher Morrison, Jeffrey Newman, Eric Nuss, Christina Peters, Taylor Pospisil, Cecile Rouelle, Tony Tyson, Rongpu Zhou, and Rafael Izquierdo. An assessment of photometric redshift pdf performance in the context of lsst. *Astronomical Society*, 2019.

Evan Schneider. Photometric redshifts and the galaxy luminosity function. *astrobites*, Jun 2011. URL <https://astrobites.org/2011/06/01/photometric-redshifts-and-the-galaxy-luminosity-function/>.

Peter Schneider. *Extragalactic Astronomy and Cosmology*. Springer-Verlag Berlin Heidelberg, 2006.

M. B. Taylor. TOPCAT and STIL: Starlink Table/VOTable Processing Software. In P. Shopbell, M. Britton, and R. Ebert, editors, *Astronomical Data Analysis Software and Systems XIV*, volume 347 of *Astronomical Society of the Pacific Conference Series*, page 29, December 2005.

A. von der Linden, M. T. Allen, D. E. Applegate, P. L. Kelly, S. W. Allen, H. Ebeling, P. R. Burchat, D. L. Burke, D. Donovan, R. G. Morris, R. Blandford, T. Erben, and A. Mantz. Weighing the Giants - I. Weak-lensing masses for 51 massive galaxy clusters: project overview, data analysis methods and cluster images. *MNRAS*, 439:2–27, March 2014. URL <https://doi.org/10.1093/mnras/stt1945>.

Wikipedia user TallJimbo. Weak gravitational lensing of galaxies in astronomy. *Wikipedia*, 2008. URL https://en.wikipedia.org/wiki/Weak_gravitational_lensing#/media/File:Shapenoise.svg.